24th INTERNATIONAL CONGRESS ON SOUND AND VIBRATION
23–27 July 2017, London

DESIGN OF ACTIVE FLUIDIC INJECTION SYSTEMS FOR JET-NOISE REDUCTION THROUGH STOCHASTIC RECONSTRUCTION OF TURBULENT FLOW FIELDS

Mattia Barbarino*, Mario Ilsami+, Raffaele Tuccillo+ and Luigi Federico*

*Italian Aerospace Research Center (CIRA), Dept. of Air Transport Environmental Impact, Capua, Italy
email: m.barbarino@cira.it

+Federico II University, Dept. of Industrial Engineering, Napoli, Italy

The prediction and reduction of noise from subsonic jets through the reconstruction of turbulent fields from Reynolds Averaged Navier-Stokes (RANS) calculations are addressed. This approach, known as Stochastic Noise Generation and Radiation (SNGR), reconstructs the turbulent velocity fluctuations by RANS fields and calculates the source terms of Vortex Sound acoustic analogy. In the first part of this work, numerical and experimental jet-noise test cases have been reproduced by means CFD RANS simulations and with different turbulence models in order to validate the approach for its subsequent use as a design tool. It was shown that the noise spectra, predicted with SNGR, are in good agreement with both the experimental data and the results of Large-Eddy Simulations (LES). In the last part of this work, an active fluid injection technique, based on extractions from turbine and injections of high pressure air in the main stream of exhaust gas, has been proposed and finally assessed with the aim to reduce the jet-noise through the mixing and breaking of the turbulent eddies. Some tests have been carried out in order to set the best design parameters in terms of mass flow rate and injection velocity and to design the system functionalities. It is shown that the SNGR method is suitable to be used for the early design phase of jet-noise reduction technologies and that a right combination of the fluid injection design parameters allow a reduction of the jet-noise up to 3.5 dB compared to the baseline case without injections.

Keywords: SNGR, RANS, LES

1. Introduction

The problem of noise generation by compressible turbulent jets has been subject of studies since the early 50s, with the introduction of the turbojet also in commercial aircraft. It has continued, even later since the 80s, with the introduction of turbofan with high bypass ratios, inherently less noisy than the previous due to the reduced exhaust velocity. In the last decades, the problem of jet noise prediction has been numerically addressed through a broad range of methods.

Despite the application of Direct Numerical Simulation (DNS) to jet-noise prediction [1-4] is becoming more feasible with the growing advancement in computational resources, due to the large disparities of length and energy scales between fluid and acoustic fields, the use of fully-solved Navier–Stokes equations without turbulence modeling (DNS) is still restricted to low Reynolds number flows.

Instead, the numerical simulation of aeroacoustics through the solution of filtered Navier Stokes equations, either using fully large-eddy simulation (LES) or hybrid RANS LES approaches such as the detached-eddy simulation (DES), is a major area of research [5-7]. However, despite the increase in computational power, even these types of simulations are not yet feasible for industrial purposes.

Indeed, industry interest is mainly devoted to reliable numerical tools to be applied to realistic configurations for re-design of old configurations and for the development of new technologies. Furthermore the growing interest on multi-disciplinary and multi-objective optimization necessarily lead to approaches that require low computational time.
Therefore, Reynolds-Averaged Navier-Stokes (RANS) simulations still remain the more feasible approach for CFD applications of industrial interest. However, RANS computations are not able to model, solely, the aeroacoustic phenomena. In this context, the stochastic approach for the prediction of noise from turbulence has received a great deal of interest in recent years. It was introduced by Kraichnan [8] and Fung [9], and it is based on the idea that Fourier components of solenoidal velocity fluctuations can be sampled in the wave-number space from a prescribed mono-dimensional energy spectrum. The revision and improvement of these methods for aeroacoustic applications have produced the stochastic noise generation and radiation (SNGR) methods [10-14]. The main goal of this paper is twofold. The first one is to make the assessment of an improved SNGR method based on the previous works of Casalino and Barbarino [13] and Di Francescantonio [14] trough the comparison with experimental and LES data of a cold subsonic jet [7]. The second one is to assess the design of an active fluid injection technique, based on extractions from turbine and injections of high pressure air in the main stream of exhaust gas. The novelty of this paper is the application of a SNGR approach for designing new devices suitable for jet noise reduction.

2. Model Description and Validation

2.1 Model description

The SNGR approach assumes that the turbulent velocity field can be reconstructed as a summation of Fourier components, according to Kraichnan [8]. Therefore, the reconstructed turbulent velocity $\boldsymbol{u}'$ at point $\boldsymbol{x}$ and time t reads:

$$\boldsymbol{u}'(x,t) = 2\sum_{n=1}^{N_F} \hat{u}_n \cos\{\boldsymbol{k}_n \cdot (\boldsymbol{x} - \varrho \boldsymbol{U} t) + \psi_n\}\sigma_n \qquad (1)$$

where $\hat{u}_n$, ψ_n e σ_n are the magnitude, phase, and direction of the nth Fourier component, respectively. As proposed by Bailly and Juvé [11], each Fourier mode is supposed to be convected at the local mean-flow velocity $\boldsymbol{U}$ corrected by the vortex convection velocity ratio ϱ. This factor may account for the wall induction effect that reduces the vortex convection velocity with respect to the mean-flow velocity at the location of the vortex core. By supposing that the turbulent flow field is isotropic, the magnitude of the n-th Fourier mode is related to the mono-dimensional energy spectrum $E(k)$ by the expression, $\hat{u}_n = \sqrt{E(k_n)\Delta k_n}$, where k_n and Δk_n are the wave number and the corresponding band of the n-th mode. The Von Kármán–Pao isotropic turbulence spectrum is assumed; that is:

$$E(k) = A(2/3)(K/k_e)(k/k_e)^4 exp[-2(k/k_\eta)][1+(k/k_e)^2]^{-17/6} \qquad (2)$$

where K is the turbulent kinetic energy, A is a numerical constant, k_e is the wave number of maximum energy, and $k_\eta = \varepsilon^{1/4}\upsilon^{-3/4}$ is the Kolmogorov wave number.
The constants A and k_e can be determined by equating the integral energy and the integral length scale derived from turbulence spectrum to the RANS quantities K and, respectively, $L_T = c_1 u'^3/\varepsilon$, being the isotropic turbulent velocity and c_1 a tuning parameter of the method. This provides $A = 1.453$ and $k_e = \frac{9\pi}{55}\frac{A}{L_T} = 0.747/L_T$.

The parameter $c_1$allows to tune the RANS turbulent integral length scale of the large-scale eddies. Its value is, by definition, close to 1, but its optimal value depends on the turbulent flow structure and conditions and on the RANS turbulence model.
The stochastic velocity perturbation field can be generated by choosing probability density functions for all the random variables involved in the Fourier decomposition.
A crucial point of the SNGR approach is the definition of the two-point space correlation of the velocity fluctuations at each node of the CFD mesh by means of an artificial numerical approach able to reproduce the physical behaviour of the turbulent structures. The simplest approach, used for instance by Bechara et al [10], would consist in segmenting the bounding box of the active source region in square paths with edges equal to the average value of the correlation length over the whole source region. Then, a set of stochastic angles are sampled in each patch and these values are finally attributed to all the mesh nodes falling in the patch. The main drawback of this approach is that the correlation length is the same over all the source region, and therefore does not account for the local Reynolds stresses and size of the turbulent structures.

The described code adopts two different SNGR approaches. The first one consists in dividing the domain in blobs which dimension is proportional to the correlation length of the CFD cells falling inside the blob and random angles are assigned constant for each blob [13] as depicted on the left of Figure 1.
The second one consists in projecting the CFD solution on an acoustic domain made of Cartesian cells which dimension is proportional to the turbulent scale length of the CFD cells falling inside the acoustic Cartesian cell (Figure 1 - right). The correlation length is assumed to be different for each Fourier mode and assumed proportional to the mode wavelength [14]. For each mode, random angles are assigned constant for the acoustic Cartesian cells having the same correlation length. The main advantage of the second approach is the reduction of the total cells to be processed in respect of the CFD mesh, although ensuring the required refinement needed.

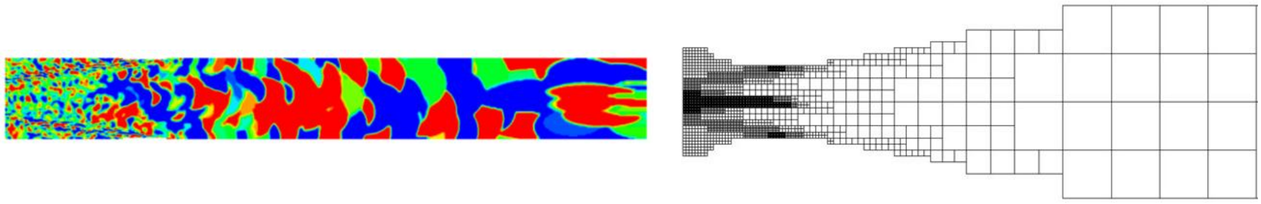

Figure 1: Two-point space correlation of a jet plume. First approach based on blobs structure (Left) - Second approach based on an adaptive Cartesian mesh (Right).

The computed velocity field is finally transformed in the frequency domain and assemble to compute the frequency counter-part of the Lamb vector $(\boldsymbol{\omega}' \times \boldsymbol{u}')$. According to the vortex-sound analogy, the far field noise is finally achieved by the Powell's equation in frequency domain:

$$p = -\rho_0 \int_V (\boldsymbol{\omega}' \times \boldsymbol{u}') \cdot \boldsymbol{\nabla} G dV \qquad (3)$$

where G is the free-field Green function and $(\boldsymbol{\omega}' \times \boldsymbol{u}')$ is the frequency counter-part of the Lamb vector.

2.2 Model validation

The SNGR approach has been firstly validated against experimental and LES results of a subsonic jet with diameter $D_j = 0.050\ m$, Mach number M = 0.75 and the Reynolds number, $Re_D = 5.0 \times 10^4$, described by Andersson [7].

A CFD RANS simulation based on the nozzle geometry used for the LES simulation [7] has been performed. The external profile of the nozzle has been reproduced by scanning from the original work [7]. The RANS simulation of the subsonic jet has been performed in the cold conditions, for which

$T_j/T_\infty = 1$, where T_j is the static temperature of the jet at the nozzle outlet section, and T_∞ is the ambient temperature.

The jet flow simulation has been carried out using the CFD software Fluent by ANSYS. The mesh extends from 0 to 50 nozzle diameters, D_j, in the axial direction. The radial extension is $10D_j$ at the nozzle outlet position and it increases up to $20D_j$ at the farfield outlet position. Mesh cells are refined in the region near the nozzle exit and in the jet shear layer zone.

A 2D axisymmetric transient pressure based second-order upwind scheme has been employed to converge fully coupled RANS equations with turbulence accounted for through *K-ε* and *K-ω SST* models. A view of the mesh made up of 1.85×10^5 cells and contour plots of the axial velocity and turbulent kinetic energy are shown in Figure 2.

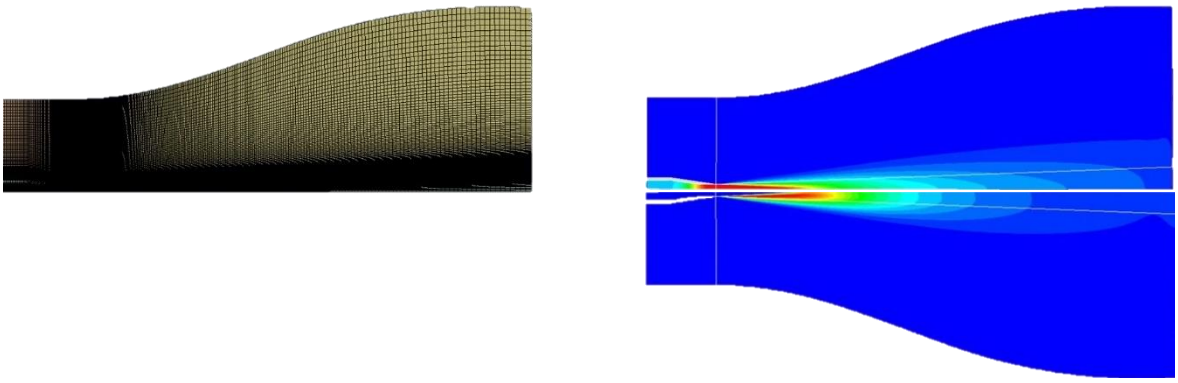

Figure 2: CFD mesh used for the RANS jet flow simulation (Left) – Contour plots of the RANS solution. Mean velocity on the top and turbulent kinetic energy on the bottom (Right).

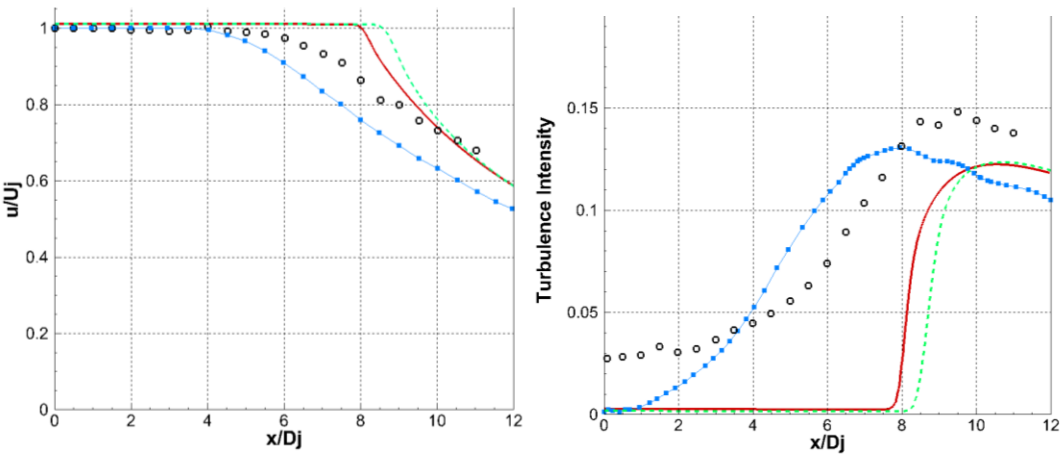

Figure 3: Centerline profile of the axial velocity (Left). Axial profiles of turbulence intensity (Rights). (Dotted black lines: experimental results, continuous red line: K-ε model, dashed green line: K-ω SST model, dotted-dashed blue line: LES).

The laminar core and the decay of the centerline velocity are in good agreement with the experimental results. The predicted laminar core length of $8D_j$ is slight higher than the experimental value as usual for RANS computations. The centerline turbulent kinetic velocity is maximum at about $10D_j$, in line with experimental results but its amplitude is slightly underestimated (Figure 3). Moreover, the *uv* correlation levels of the radial velocity profile are underestimated by the RANS analysis due to lower mixing predicted and overestimated by the LES (Figure 4).

It can be argued that the RANS analysis results are in fairly good agreement with experimental data and LES results although they underestimate the value of *uv* correlation and do not predict the gradual increase of turbulent energy in the region of the laminar core.

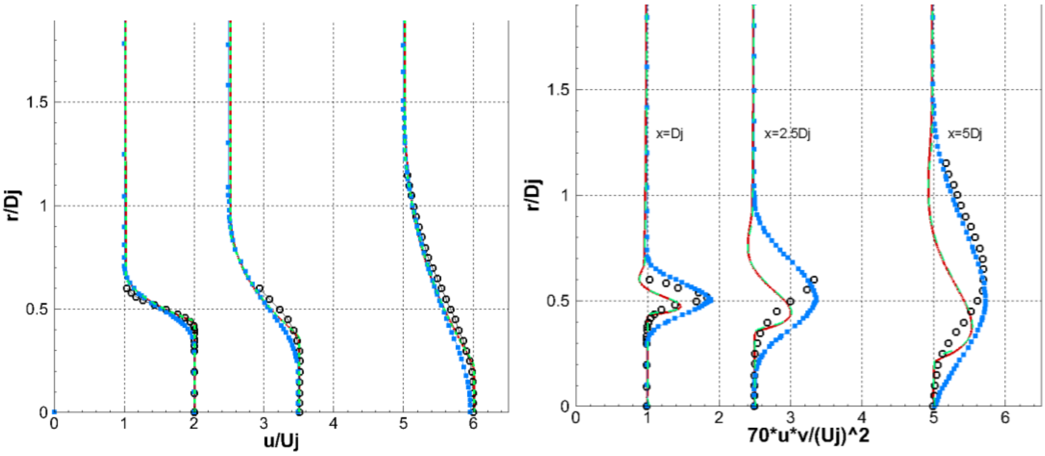

Figure 4: Radial profiles of axial velocity (Left). Radial profiles of uv correlation (Right). The profiles have been staggered according to their axial location. (Dotted black lines: experimental results, continuous red line: K-ε model, dashed green line: K-ω SST model, dotted-dashed blue line: LES).

The acoustic field is evaluated by processing the RANS data by means the SNGR approach. To compute the stochastic noise sources, the axisymmetric CFD solution has been initially projected on a 3-D domain. The noise has been computed directly from the Fourier transform of the Lamb vector by using the integral solution of Powell's equation. Acoustic results are computed on a total of 25 microphones on two microphones arcs in the jet far-field region and compared against LES and experimental results. 14 microphones are arranged on a first arc of radius $30D_j$ from the center of the nozzle outlet section and positioned by 20 degrees to 150 degrees with an angular steps of 10 degrees. The remaining 11 microphones were placed on a second arc of radius $50D_j$ from the center of the nozzle outlet section and positioned by 50 degrees to 150 degrees with an angular step of 10 degrees. The acoustic results are expressed in terms of the PSD (Power Spectral Density) and OASPL (Over-All Sound Pressure Level).

SNGR method does not take account for either convective effects or refractions by the shear layer. Therefore, SNGR results have been corrected, as suggested by Lighthill [15], to account for convective effects by using a Doppler factor of $1/(1-M_c cos\theta)^{\alpha}$, where α is a proper exponential coefficient and M_c is the convective Mach number. In this work α is assumed equal to 4 and applied for the PSD correction, thus, the OASPL has been computed starting from the corrected PSD. Furthermore, in a first approximation, mean flow refraction effects have been neglected.

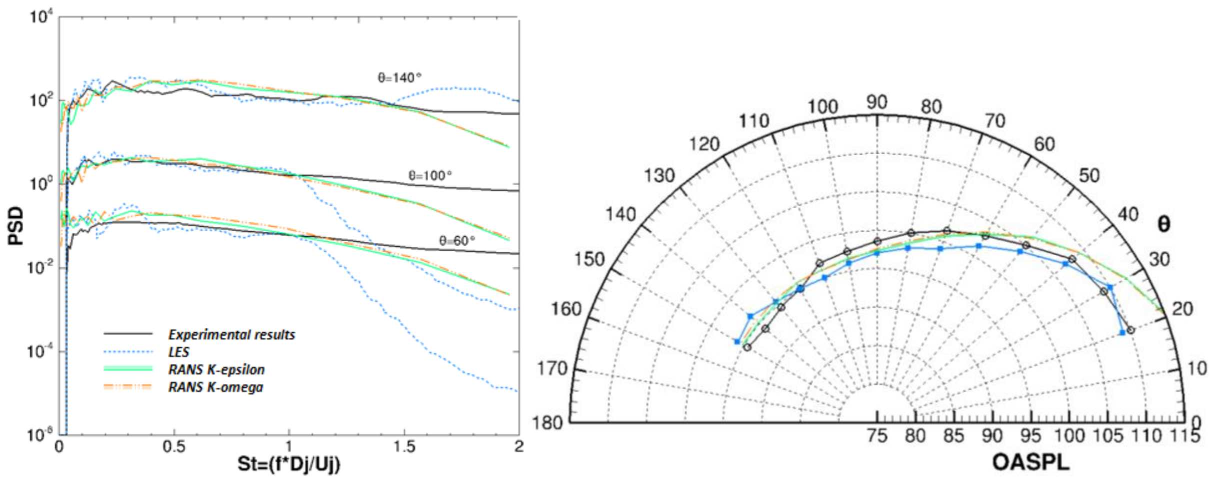

Figure 5: Power spectra of far-field pressure signal for a few observer locations on the inner arc, $30D_j$ (Left). The PSD spectra have been staggered by multiplying the amplitude by a factor 10^{2n}, where $n = \left(\frac{\theta-20}{40}\right)$ and θ being the angle from the jet axis. Overall Sound Pressure Level Directivity (Right).

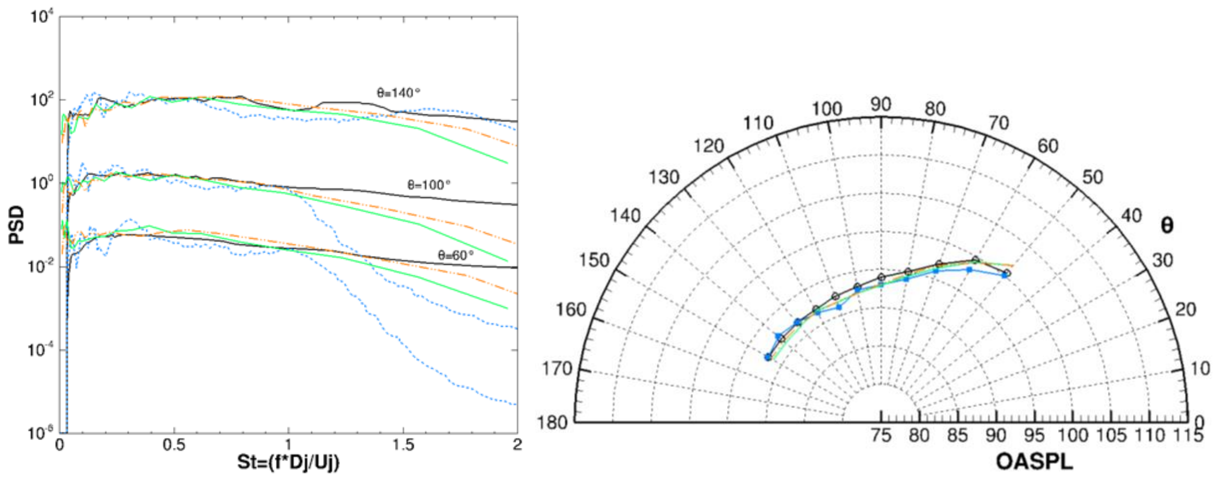

Figure 6: Power spectra of far-field pressure signal for a few observer locations on the outer arc, $50D_j$ (Left). The PSD spectra have been staggered by multiplying the amplitude by a factor 10^{2n}, where $n = \left(\frac{\theta-20}{40}\right)$ and θ being the angle from the jet axis. Overall Sound Pressure Level Directivity (Right).

Finally, Figure 5 and Figure 6 depict acoustic results for both arcs in terms of PSD spectra and OASPL levels showing that SNGR results are in very good agreement with the experimental results and LES analyses.

3. Active Fluidic Injection System

In this section, an experimental technology for reducing the jet noise based on a fluidic injection is assessed by means of the SNGR approach and applied to the jet analyzed in the Section 2.2. Several experimental studies, conducted over the last decades, have shown that the fluid injection technique effectively allows to reduce the noise from turbulence [16-18]. Therefore, the technological solution, proposed here, basically consists in injecting small jets of secondary air into the main flow which comes out from the nozzle of the jet engine exhaust (Figure 7). This secondary air jet is derived from gas bleeding from the turbine which is located immediately upstream of the nozzle.

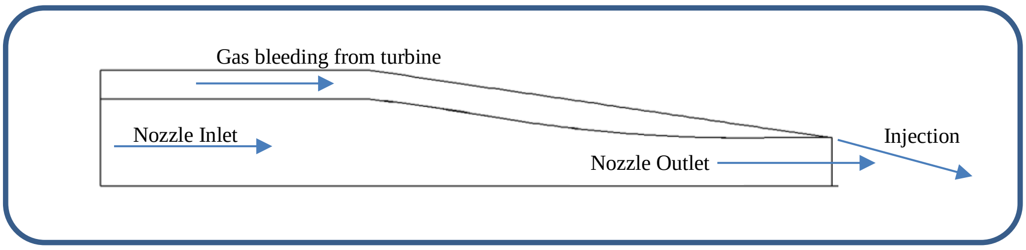

Figure 7: Sketch of the active Fluidic Injection System

Two injection mass flow rate values are considered, corresponding about to 5% and 10% of the total mass flow rate of the turbine. A maximum rate of about 10% has been used in order to preserve the nominal turbine power, whereas, pressure and temperature of the drained mass flow rate have been computed, assuming to be greater than the ambient conditions and according to the thermodynamic expansion. Two injection sections with a total area of around 4% and 10% of the nozzle outlet area have been considered and modelled in the computational domain and corresponding respectively to the 5% and 10% of the turbine mass flow rate. Finally, the spray conditions have been evaluated at three different injections angles equal to 45, 60 and 80 degrees. The following test matrix has been, thus, assembled for the RANS+SNGR analyses. Examples of the different turbulence levels obtained by varying the injection patterns are displayed in Figure 8.

Table 1: Test matrix for the injection system design.

TEST	***Injection mass flow rate / Nozzle mass flow rate***	***Injection section area / Nozzle outlet area***	***Injection Direction [deg]***	***Injection Velocity [m/s]***
1	13.0 %	10.2 %	45	350
2	13.0 %	10.2 %	60	450
3	13.0 %	10.2 %	80	690
4	6.5 %	4.08 %	80	720

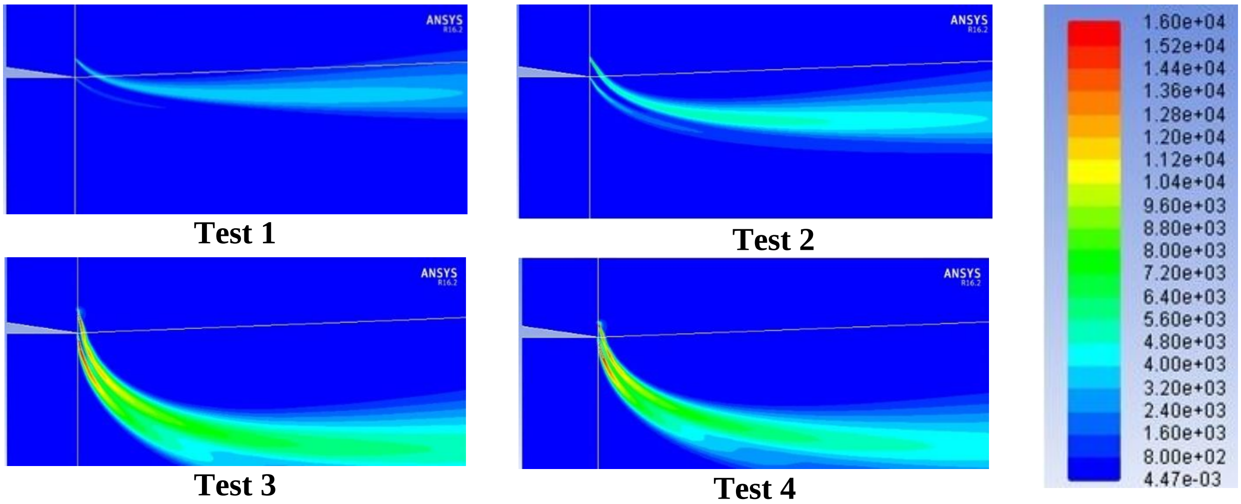

Figure 8: Turbulent kinetic energy levels [m^2/s^2], for the injection patterns tested.

Finally, Figure 9 shows the directivity patterns achieved with the tested fluidic injection system. It has been observed that the fluid injection technique seems to produce a reduction of the OASPL compared to the baseline condition in all the 4 tests analyzed. In particular, in the fourth test condition the maximum reduction of the OASPL, of about 3.5 dB, is observed at each directivity angle.

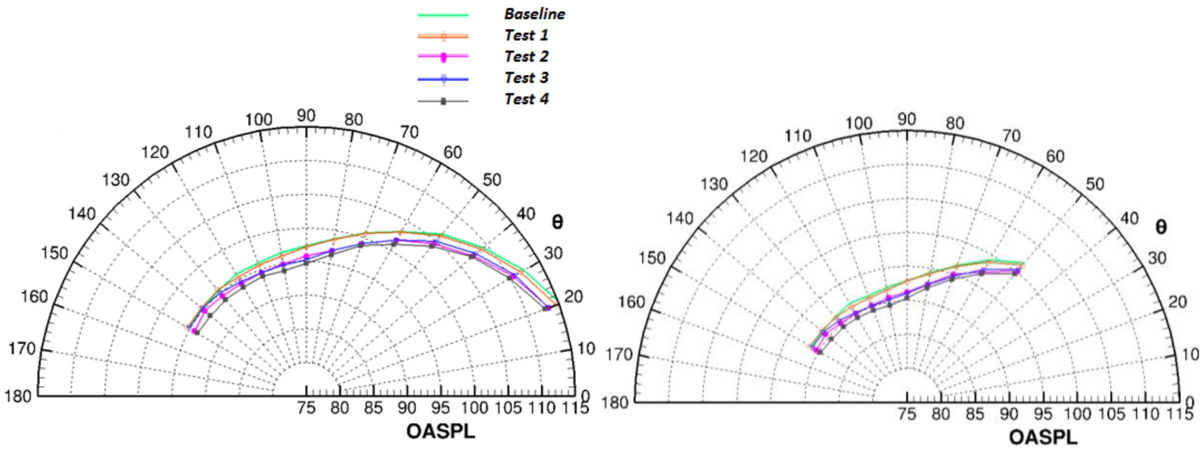

Figure 9: Overall Sound Pressure Level Directivity on the inner arc (Left) and on the outer arc (Right).

5 Conclusions

This paper illustrated the use of a computational aeroacoustics approach, named SNGR, based on CFD RANS solutions, and aimed to the jet-noise prediction and reduction.

In the first part of this work, the coupled RANS-SNGR approach has been successfully assessed and validated against both experimental data and results of Large-Eddy Simulations (LES).

In the second part, a technique based on the injecting of small jets of secondary air into the main jet flow, and drained from the turbine, is proposed and assessed. It has been shown that the fluid injection technique allows to effectively reduce the jet noise. Moreover, as forecasted by the parametric study hereby showed, the fluid injection technique can be designed as an active system, after a proper optimization of several parameters, like the drained mass flow rate, the related pressure and temperature, the injection section area and jet angle, depending on the flight and engine conditions.

REFERENCES

1 Colonius, T., Lele, S. K. & Moin, P. "Sound generation in a mixing layer", *J. Fluid Mech.*, **330**, 375-409, (1997).

2 Colonius, T., Mohseni, K., Freund, J. B., Lele, S. K., Moin, P. "Evaluation of noise radiation mechanisms in a turbulent jet", *Center for Turbulence Research, Proceedings of the Summer Program* ,159-167 (1998).

3 Freund, J., "Noise Sources in a Low-Reynolds-number Turbulent Jet at Mach 0.9", *J. Fluid Mech.*, **438**, 277-305, (2011).

4 Mitchell, B., Lele, S., and Moin, P., "Direct Computation of the Sound Generated by Vortex Pairing in an Axisymmetric Jet", Journal of Fluid Mechanics, **383**, 113-142, 1999.

5 Bogey, C., Bailly, C., and Juvè, D., "Computation of the Sound Radiated by a 3-D Jet Using Large Eddy Simulation", *Proceedings of the 6th AIAA/CEAS Aeroacoustics Conference*, (2000).

6 Mankbadi, R., Shih, S., Hixon, R., and Povinelli, L., "Direct Computation of Jet Noise Produced by Large-Scale Axisymmetric Structures", *J. Propulsion and Power*, **16**, No. 2, 207-215, (2000).

7 Andesson, N., Eriksson, L.E., Davidson, L., "A Study of Mach 0.75 Jets and Their Radiated Sound Using Large-Eddy Simulation", *Proceedings of 10th AIAA/CEAS Aeroacoustics Conference*, (2004).

8 Kraichnan, R., H., "Diffusion by a Random Velocity Field", *Physics of Fluids*, **13**, No. 1, 22–31, (1970).

9 Fung, J., C., H., Hunt, J., C., R., Malik, N., A., and Perkins, R., J., "Kinematic Simulation of Homogeneous Turbulence by Unsteady Random Fourier Modes", *J. Fluid Mech.*, **236**, 281–318 (1992).

10 Béchara,W., Bailly, C., Lafon, P., and Candel, S., "Stochastic Approach to Noise Modeling for Free Turbulent Flows", *AIAA Journal*, **32**, No. 3, 455–464, (1994).

11 Bailly, C., and Juvé, D., "A Stochastic Approach to Compute Subsonic Noise Using Linearized Euler's Equations", *Proceedings of 5th AIAA/CEAS Aeroacoustics Conference*, (1999).

12 Billson, M., Eriksson, L., and Davidson, L., "Jet Noise Modeling Using Synthetic Anisotropic Turbulence", *Proceedings of 10th AIAA/CEAS Aeroacoustics Conference*, (2004).

13 Casalino, D., Barbarino, M., "Stochastic Method for Airfoil Self-Noise Computation in Frequency-Domain", *AIAA Journal*, **49**, No. 11, 2453-2469 (2011).

14 Di Francescantonio, P., "Side Mirror Noise with Adaptive Spectral Reconstruction", *Proceedings of SAE 2015 Noise and Vibration Conference and Exhibition*, (2015).

15 Lighthill, M. J., "Jet Noise", *AIAA Journal*, **1**, No. 7, 1507–1517, (1963).

16 Henderson, B.S., Kinzie, K.W., Whitmire, J., and Abeysinghe, A., "The impact of fluidic chevrons on jet noise", *Proceedings of 11th AIAA/CEAS Aeroacoustics Conference,* (2005).

17 Kinzie, K.W., Henderson, B.S., Whitmire, J., and Abeysinghe, A., "Fluidic chevrons for jet noise reduction", *Proceedings of the 2004 International Symposium on Active Control of Sound and Vibration (ACTIVE 2004),* (2004).

18 Henderson, B.S., Kinzie, K.W., Whitmire, J., and Abeysinghe, A., "Aeroacoustic Improvements to Fluidic Chevron Nozzles", *Proceedings of 12th AIAA/CEAS Aeroacoustics Conference*, (2006).